Self-Gating Effect in the Electron Y-Branch Switch

Jan-Olof J. Wesström

The Laboratory of Photonics and Microwave Engineering, Department of Electronics, Royal Institute of Technology,
Electrum 229, S-164 40 Kista, Sweden

In an electron waveguide Y-branch switch the electrostatic field applied between two gates switches a current into either of two branches. A novel mode of operation is proposed. For finite source-drain potentials, the switching field is shown to be strongly influenced by the electrochemical potentials in the waveguides. For certain biasing schemes this can be used to achieve gain without external gates and their *RC* constants. This allows switching up into the THz range in this new class of gateless mesoscopic devices. Conditions for bistability and oscillation are derived. [S0031-9007(99)08629-9]

PACS numbers: 73.50.Mx, 72.15.–v

The electron Y-branch switch (YBS) [1] is a so-called electron waveguide device (EWD), which has been considered as a candidate for future very low power, high speed electronics. As an advantage versus other EWDs such as the Aharonov-Bohm interferometer [2], the directional coupler [3], and the quantum stub transistor, [4] the YBS benefits from a monotonic response facilitating the implementation of logic functions [5]. In an electron Y-branch switch (Fig. 1), an electric field can direct electrons, into either of two branches, while the other branch is cut off. In simulations [6,7] it has been shown that if the waveguides of the YBS have only one populated subband, a sufficient lateral field is created by applying a voltage of a few mV between the gates on both sides and that the switching is very efficient for a wide range of electron energies. This somewhat surprising behavior is due to the fact that the electrons do not have to be stopped by a barrier. The device does not have to be depleted anywhere. Instead, the electrons are merely deflected into either of the arms by the lateral field. The same phenomenon is predicted to yield the interesting possibility of using switching voltages below $k_B T/e$, offering low power consumption. At the cryogenic temperatures typical of present day mesoscopic experiments, however, the switching voltage is larger than the very low $k_B T/e$ due to a quantum limitation [Eq. (3)]. The electric field in these simulations was, however, calculated in the absence of voltages between the reservoirs. As Landauer pointed out [8] the fields created at a scatterer are often important, when we leave equilibrium. *The present Letter therefore estimates the effects of finite differences between the electrochemical potentials in the reservoirs including the effects of induced space charge inside the device and comes to the conclusion that these affect the lateral field and thus the switching much more than the gate voltages do.*

The simulations showed that the reflections in the stem waveguide were very small. Neglecting these and making use of the unitarity and reciprocity of coherent transport in the absence of magnetic fields [9], the transmission probability matrix takes the form

$$\mathbf{T}_Y = \begin{bmatrix} 0 & \frac{1+\gamma}{2} & \frac{1-\gamma}{2} \\ \frac{1+\gamma}{2} & \frac{(1-\gamma)^2}{4} & \frac{1-\gamma^2}{4} \\ \frac{1-\gamma}{2} & \frac{1-\gamma^2}{4} & \frac{(1+\gamma)^2}{4} \end{bmatrix}, \quad (1)$$

as reported in [5]. Neglecting the potential difference between the reservoirs, the switching parameter γ had a dependence on the field between the gates which can for simplicity be approximated by

$$\gamma = \tanh \frac{\eta_g \Delta V_g}{\Delta V_s}, \quad (2)$$

where ΔV_g is the voltage between the gates. The gating efficiency η_g, estimated in this Letter, is a measure of how well the electrostatic potential difference *in the waveguides* ΔV_{23} follows the gate voltage. The switching voltage ΔV_s is a measure of how large a change in ΔV_{23} is required to affect γ. It is fundamentally limited by the Heisenberg relation between interaction time and energy,

$$e\Delta V_s \approx \frac{\hbar v_F}{L_i}, \quad (3)$$

where v_F is the Fermi velocity and L_i is the interaction length (Fig. 1).
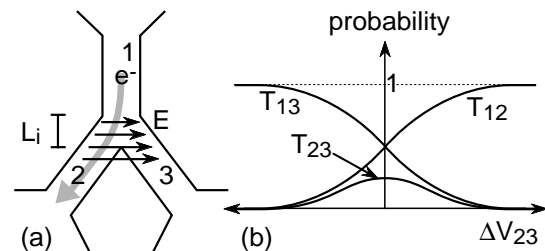

FIG. 1. (a) In the Y-branch switch an electric field deflects the electrons from the stem (1) into either of the branches (2 or 3). The field is caused by a voltage applied between external gates, or by the potential difference between the waveguides themselves. (b) The transmission probabilities Eq. (1) vary with the electrostatic potential difference between the two waveguides.

The difference in electrochemical potential between waveguides 2 and 3, $\Delta\mu_{23}$, creates a charge buildup which in turn creates a difference in electrostatic potential, ΔV_{23}, between the waveguides, which corresponds to a lateral field superposed to the one from the gate electrodes. The resulting field controls the switching parameter γ.

$$\gamma = \tanh \frac{\eta_g \Delta V_g + \eta_{sg} \frac{\Delta\mu_{23}}{-e}}{\Delta V_s} . \qquad (4)$$

Before discussing the resulting nonlinearity in conductance and some interesting applications for this self-gating effect, we will first attempt to assess the value of both the gate efficiencies η_g and η_{sg}, and argue that the self-gating is the dominant gating mechanism.

In a metal structure with a high density of states (DOS), a variation of the electrochemical potential implies a corresponding change in the electrostatic potential, $\Delta V = \Delta\mu / -e$. The question is what happens in single mode electron waveguides with a limited DOS. We will assess η_g and η_{sg} by estimating the electrostatic potential difference between the waveguides $\Delta V_{23} = \Delta V_2 - \Delta V_3$ as a function of the electrochemical potential difference $\Delta\mu_{23} = \Delta\mu_2 - \Delta\mu_3$ between the waveguides and of the applied gate voltage $\Delta V_g = \Delta V_{g2} - \Delta V_{g3}$. To simplify, the only capacitive couplings taken into account are those between a gate and the waveguide closest to it, C_{g2} and C_{g3}, and the one between the two waveguides C_{23}. The device is symmetric so $C_{g2} = C_{g3} = C_g$. The charge induced in waveguide 2 is

$$\Delta\rho_2 = C_{23}(\Delta V_{23}) + C_{g2}(\Delta V_2 - \Delta V_{g2}). \qquad (5)$$

For the electrochemical potentials in the waveguide, we have

$$\Delta\mu_2 = -e\left(\Delta V_2 + \frac{\Delta\rho_2}{C_Q}\right), \qquad (6)$$

where $C_Q = e^2 \times$ DOS is the "quantum capacitance." From the above equations and the corresponding equations for waveguide 3, it is straightforward to express ΔV_{23} in terms of the gate voltage ΔV_g and the difference in electrochemical potential in the waveguides $\Delta\mu_{23}$

$$\Delta V_{23} = \frac{C_g \Delta V_g + C_Q \frac{\Delta\mu_{23}}{-e}}{C_Q + C_g + 2C_{23}} . \qquad (7)$$

We can now identify η_g and η_{sg}

$$\begin{aligned} \eta_g &= \frac{C_g}{C_Q + C_g + 2C_{23}} , \\ \eta_{sg} &= \frac{C_Q}{C_Q + C_g + 2C_{23}} . \end{aligned} \qquad (8)$$

For single-mode electron waveguides, the quantum capacitances are usually larger than the geometric ones. We have

$$C_Q = \frac{e^2 m^*}{\hbar \pi k_F} = \frac{2}{v_F R_0} , \qquad (9)$$

where k_F is the Fermi wave vector and m^* is the effective electron mass. $R_0 = \pi\hbar/e^2 \approx 13$ kΩ. The ordinary, geometry dependent capacitances per unit length are seldom more than a small factor A from the dielectric constant of the material,

$$C_{geo} = A\epsilon_0\epsilon_r . \qquad (10)$$

The ratio between these types of capacitances can therefore be expressed as

$$\frac{C_Q}{C_{geo}} = \frac{8\alpha}{A\epsilon_r} \frac{c}{v_F} , \qquad (11)$$

where $\alpha \approx 1/137$ is the fine-structure constant and c is the velocity of light. This means that for realistic parameters, for example $A = 2$, $\epsilon_r = 10$, the capacitance ratio [Eq. (11)] is larger than unity up to Fermi velocities around $v_F \approx 10^6$ m/s. It also means that according to Eq. (8) self-gating is the dominant gating mechanism up to this velocity and η_{sg} is close to unity up to $v_F \approx 3 \times 10^5$ m/s, so the electrostatic potential difference ΔV_{23} closely follows the electrochemical potentials in the waveguides, implying that we can exploit the low fundamental limit on switching voltage [Eq. (3)]. Numerical simulations will, however, be necessary to calculate the geometry-dependent self-consistent charge and field distributions for finite potentials between the reservoirs, from which we more accurately may deduce η_g, η_{sg}, and ΔV_s. The conclusion from this brief analysis must, however, be that the difference in electrochemical potential between waveguides 2 and 3 affects the switching more than the gate potentials.

The phenomenon creates a nonlinearity in the conductance between the three leads, and we will now examine how this can be exploited without a gate voltage or if the gate electrodes are excluded from the device $\Delta V_g = 0$.

First, we note that the self-switching is governed by $\Delta\mu_{23}$, that is the electrochemical potential difference between the electron waveguides 2 and 3 close to the junction. This may differ from the difference in potential between the reservoirs. The conductance matrix [9]

$$\mathbf{G}^r = \frac{1}{R_0} (\mathbf{E} - \mathbf{T}_Y), \qquad (12)$$

where $\mathbf{E}$ is the identity matrix, relates the currents $\bar{I}$ into the waveguides with the potentials $\bar{\mu}^r$ *in the reservoirs*. $\bar{I} = \mathbf{G}^r \bar{\mu}^r / -e$. By discounting the contact resistances of $R_0/2$ between each waveguide and its reservoir, we get a relation between the current and the potential $\bar{\mu}$ *in the waveguides*.

$$\mathbf{G} = \frac{2}{R_0} (\mathbf{E} + \mathbf{T}_Y)^{-1}(\mathbf{E} - \mathbf{T}_Y). \qquad (13)$$

In [10] it was shown that this conductance relation is valid for frequencies $\omega \ll 1/\tau_{tr}$, where τ_{tr} is the transit time for an electron between the points close to the junction where the potentials $\bar{\mu}$ are considered. Separating the

contact resistances from the conductance matrix of the actual junction it is thus possible to model the I-V characteristics of the device with an equivalent circuit, as in Fig. 2. Inserting the transmission probability matrix $\mathbf{T}_Y$ [Eq. (4)] and simplifying, we obtain

$$\mathbf{G} = \frac{2}{R_0(1 - \gamma^2)}$$
$$\times \begin{bmatrix} 2(1 + \gamma^2) & -(1 + \gamma)^2 & -(1 - \gamma)^2 \\ -(1 + \gamma)^2 & (1 + \gamma)^2 & 0 \\ -(1 - \gamma)^2 & 0 & (1 - \gamma)^2 \end{bmatrix}.$$
$$(14)$$

We will now examine the behavior of the device when the biasing is symmetric, i.e., the potentials of reservoirs 2 and 3 are the same. For convenience, we set the potentials of the reservoirs to $\mu_2^r = \mu_3^r = 0$ and $\mu_1^r < 0$. Then a positive current will flow into waveguide 1. This current will be partitioned into waveguides 2 and 3, depending on the switching parameter γ. Because of the contact resistance (Fig. 2), a difference in current will create a difference in electrochemical potential between waveguides 2 and 3, $\Delta\mu_{23}$. This will in turn affect γ through Eq. (4) so that the current is directed to the waveguide with *lower* electrochemial potential, which further reduces that potential. The result is a bistability, where the current is directed to either of the branches depending on the state of the device. Whether the bistability occurs or not depends on the value of μ_1^r. According to Eqs. (1) and (12), the current into lead 2 becomes $(1 + \gamma)\mu_1^r/2eR_0$. Because of the contact resistance a potential in waveguide 2 of $\mu_2 = (1 + \gamma)\mu_1^r/4$ is produced. In the same manner μ_3 can be calculated, yielding

$$\Delta\mu_{23} = \Delta\mu_2 - \Delta\mu_3 = \gamma\mu_1^r/2. \qquad (15)$$

If we plot this relation along with Eq. (4), as in Fig. 3, we see that we get three solutions, $\gamma = 0$ and $\gamma \approx \pm 1$, if $\mu_1^r < -2eV_s/\eta_{\text{sg}}$. According to the intuitive arguments above, $\gamma \approx \pm 1$ are stable solutions while $\gamma = 0$ is not. For $\mu_1^r > -2eV_s/\eta_{\text{sg}}$ there is only one solution. A useful hydrodynamical analogy, where the bistability is evident, is given in Fig. 3(b).

An alternative to bistability, however, is that, for certain conditions, the flap may start oscillating, like the reed in the mouthpiece of a woodwind instrument, e.g., a clarinet. The same thing is true for the self-gated YBS. The counterintuitive fact that a lower electrochemical potential, for example in waveguide 2, may lead to an increase of the current from the junction into that waveguides can, as we will see, be represented by a negative differential conductance (NDC) between waveguides 2 and 3. It is well known that an NDC may yield an oscillation if the load has appropriate reactive properties and a dissipative component that is not too high. For the hydrodynamic analogy, this is accomplished by the propagation delay of the sound waves in tubes 2 and 3, together with the negative reflection coefficient at the ends of those tubes. We will see that under some conditions this is also the case for the device under consideration, since the sound waves have an equivalent in the one-dimensional plasma waves in the electron waveguides, but first we investigate the NDC.

To estimate the NDC, we linearize around a bias point where $\mu_2 = \mu_3$ and $\gamma = 0$, i.e., the unstable solution. To find the operating point we first note that we, according to Eq. (1), have no reflection in waveguide 1. This means that the current into that waveguide is $\mu_1^r/(-eR_0)$. From (Fig. 2) we immediately get $\mu_1 = \mu_1^r/2$ and $\mu_2 = \mu_3 = \mu_1^r/4$ since this current is split in two equal halves when $\gamma = 0$. We now investigate the current when we introduce a small deviation $\mu_2 = \mu_1^r/4 + \delta\mu$, $\mu_3 = \mu_1^r/4 - \delta\mu$. The excitation is antisymmetric since the loads (e.g., the contact resistances) are assumed equal and $I_2 + I_3$ is constant. Inserting these potentials into Eq. (14), we obtain

$$I_2 = \frac{2}{R_0}\frac{1 + \gamma}{1 - \gamma}\left(\frac{\delta\mu}{-e} - \frac{\mu_1^r}{-4e}\right), \qquad (16)$$

where γ is given by Eq. (4) with $\Delta\mu_{23} = 2\delta\mu$ and $\Delta V_g = 0$. Linearizing we obtain the differential conductance G_n,

$$G_n = \frac{-e\delta I_2}{\delta\mu} = \frac{2}{R_0}\left(1 + \frac{\eta_{\text{sg}}\mu_1^r}{e\Delta V_s}\right). \qquad (17)$$
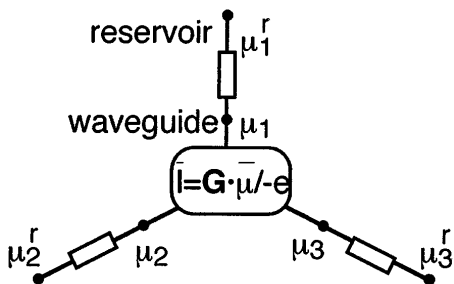

FIG. 2. Since we need to consider the electrochemical potentials *inside* the waveguides, it is convenient to separate the contact resistances of $R_0/2$ from the conductance of the actual junction $\mathbf{G}$.
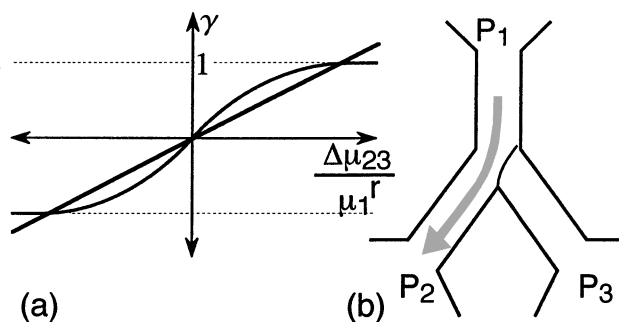

FIG. 3. (a) Equations (4) and (15). (b) Hydrodynamic analogy of the self-gated Y-branch switch. A water flow is directed by the flap, which in turn is bent by the difference in pressure between the pipes.

This constitutes a NDC already at $\mu_1^r < -e\Delta V_s/\eta_{sg}$. We will now see how waveguides 2 and 3 may act as resonators for an oscillation. In [11], the high frequency properties of electron waveguides were described in terms of propagating plasma waves. A microwave-engineering approach, where the plasma waves were modeled as voltage waves on equivalent transmission lines, was developed. The Fermi velocity v_F and the screening by a nearby metallic plane, e.g., the commonly used split gates, were found to be the main parameters influencing the plasma wave propagation velocity $u > v_F$ and a characteristic impedance, $Z_Q > R_0/2$, in the transmission-line model. Also, the boundary condition for these waves at the interfaces to the reservoirs was calculated. In the transmission-line model, it was represented by a series resistance of $R_0/2$. Using these results from [11] we obtain a model of waveguides 2 and 3, as in Fig. 4. At an oscillation frequency of

$$f = u/(4L), \tag{18}$$

the length of the waveguides L corresponds to a quarter wave, and the waveguides can be considered as quarter-wave transformers, well known from microwave engineering. The load impedance at the reservoir $R_0/2$ can then be transformed to an impedance at the junction $Z_j = Z_Q^2/(R_0/2)$, which will be connected in parallel with the negative conductance of the junction. The requirement for oscillation to start is that the total conductance $G_n + Z_j^{-1} < 0$. This can be expressed as

$$\frac{\eta_{sg}\mu_1^r}{-e\Delta V_s} > 1 + \left(\frac{R_0/2}{Z_Q}\right)^2. \tag{19}$$

For a plasma velocity of $u = 4 \times 10^5$ m/s and a waveguide length of $L = 1 \times 10^{-7}$ m, the oscillation frequency becomes $f = 1$ THz. Reducing the length of the waveguides used as resonators, f increases, but another time constant, the transit time through the junction limits the maximum frequency, since the electron has to travel through the whole interaction length L_i in the same field, to be deflected properly. The Fermi velocity is limited in a single-mode waveguide, since a higher Fermi energy would populate the second subband. If we for simplicity assume an infinite rectangular potential profile we obtain a maximum Fermi velocity of $v_F < \sqrt{3}\pi\hbar/wm^*$ before the second subband is populated. The width of the waveguide is denoted w. For the transit time we then obtain

$$\tau_{tr} = \frac{L_i}{v_F} > \frac{L_iwm^*}{\sqrt{3}\pi\hbar}, \tag{20}$$

implying a square dependence on the length scale. Already at $L_i = 70$ nm, and $w = 20$ nm this corresponds to $\tau_{tr} \approx 0.1$ ps assuming an effective mass of $m^* = 0.04m_0$. The main reason for the high frequency is the absence of
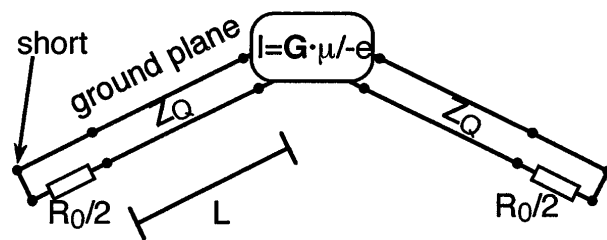

FIG. 4. The small-signal high-frequency properties of waveguides 2 and 3 may be represented by a transmission line analogy, where the extra wire is a representation of the metal ground plane. The high frequency impedance of the voltage supplies are represented by shorts since they are assumed to be very low in comparison with $R_0/2$.

gates and the large RC constants intrinsic to the highly resistive EWDs.

Experimentally, the high frequency oscillations may be difficult to detect inside a cryostat. The bistability is a dc effect and easier to study by, for example, monitoring the currents while the potential difference $\mu_2^r - \mu_3^r$ is swept. The oscillations must then, however, be suppressed by reducing Z_Q, placing the screening metal plane close to the waveguides [11].

Another interesting possibility is to leave reservoir 1 floating and measure μ_1^r while μ_2^r and μ_3^r are varied. From the analogy of Fig. 3(b) we then see that waveguide 1 will connect in a resistanceless fashion to the branch with lower μ, and μ_1^r will tend to take the lower value of μ_2^r and μ_3^r. This can also be used as a primitive logic gate ($\mu_1^r = \mu_2^r$ OR μ_3^r). By dynamically connecting waveguide 1 to either of the branch waveguides depending on which one momentarily has the lower electrochemical potential, we can also overcome a fundamental difficulty associated with electron waveguides; it is impossible to connect three single-moded electron waveguides in a resistanceless junction (even if we discount the contact resistances). This advantage should have applications in future electron-waveguide circuits, along with the bistability and oscillatory behavior discussed in this Letter.

[1] T. Palm, J. Appl. Phys. **74**, 3551 (1993).
[2] S. Datta, Superlattices Microstruct. **6**, 83 (1989).
[3] J. A. del Alamo and C. C. Eugster, Appl. Phys. Lett. **56**, 78 (1990).
[4] F. Sols, M. Macucci, U. Ravaioli, and K. Hess, J. Appl. Phys. **66**, 3892 (1989).
[5] T. Palm and L. Thylén, J. Appl. Phys. **79**, 8076 (1996).
[6] T. Palm, L. Thylén, O. Nilsson, and C. Svensson, J. Appl. Phys. **74**, 687 (1993).
[7] T. Palm and L. Thylén, Appl. Phys. Lett. **60**, 237 (1992).
[8] R. Landauer, IBM J. Res. Dev. **32**, 306 (1988).
[9] M. Büttiker, Phys. Rev. Lett. **57**, 1761 (1986).
[10] J.-O. J. Wesström, Phys. Rev. B **58**, 10 351 (1998).
[11] J.-O. J. Wesström, Phys. Rev. B **54**, 11 484 (1996).